

Provided for non-commercial research and education use.  
Not for reproduction, distribution or commercial use.



This article appeared in a journal published by Elsevier. The attached copy is furnished to the author for internal non-commercial research and education use, including for instruction at the authors institution and sharing with colleagues.

Other uses, including reproduction and distribution, or selling or licensing copies, or posting to personal, institutional or third party websites are prohibited.

In most cases authors are permitted to post their version of the article (e.g. in Word or Tex form) to their personal website or institutional repository. Authors requiring further information regarding Elsevier's archiving and manuscript policies are encouraged to visit:

<http://www.elsevier.com/copyright>



## Formation of nanocrystals due to giant-fault deformation in Gum Metals

S.V. Bobylev,<sup>a,b</sup> T. Ishizaki,<sup>c</sup> S. Kuramoto<sup>c</sup> and I.A. Ovid'ko<sup>a,b,\*</sup>

<sup>a</sup>*Institute of Problems of Mechanical Engineering, Russian Academy of Sciences, Bolshoj 61, Vas. Ostrov, St. Petersburg 199178, Russia*

<sup>b</sup>*Department of Mathematics and Mechanics, St. Petersburg State University, St. Petersburg 198504, Russia*

<sup>c</sup>*Toyota Central Research and Development Laboratories Incorporated, Nagakute, Aichi 480-1192, Japan*

Received 15 March 2011; revised 30 June 2011; accepted 4 July 2011

Available online 13 July 2011

A special micromechanism for stress-driven formation of nanocrystals (nanoscale grains) in Gum Metals (new Ti-based alloys with remarkable mechanical properties) is suggested and theoretically described. Within our description, intersection of giant faults – carriers of highly localized plastic deformation – and grain boundaries (GBs) induces transformations of GBs. These transformations lead to formation of nanocrystals and delocalization of plastic flow in Gum Metals. The theoretical results account for corresponding experimental data reported in the literature.

© 2011 Acta Materialia Inc. Published by Elsevier Ltd. All rights reserved.

**Keywords:** Titanium alloys; Gum Metals; Plastic deformation; Disclinations

Nanoscale deformation processes associated with stress-driven transformations of grain boundaries (GBs) in various materials represent the subject of intensive research (see, e.g. [1–4]). Commonly the stress-driven transformations include GB migration, grain growth and nucleation of new grains during plastic deformation of solids; see, e.g. [1–17]. Recently, unusual, stress-driven transformations of GBs have been experimentally documented in plastically deformed Gum Metals [18–20], a new group of special alloys with Ti-24 at.% (Ta + Nb + V)–(Zr–Hf)–O composition and remarkable properties. Following Refs. [18–20], extra large GB steps are formed when GBs are intersected by giant faults – extended planar defects having thickness of around 1 nm and conducting very large local plastic strain of thousands percent or more – in Gum Metals. The GB steps have a typical length of around 500–1000 nm [18–20]. Also, nanocrystals (nanoscopic regions with crystal lattices misoriented relative to the neighboring lattice) are formed in their vicinities [19,20]. The micromechanism for formation of the nanocrystals near the GB steps produced by giant-fault

deformation in Gum Metals is unclear. At the same time, this phenomenon is of significant importance for understanding the nature of plastic deformation processes in Gum Metals and their remarkable mechanical properties (high strength, excellent cold workability, superelasticity; see, e.g. [18–20]). The main aim of this paper is to suggest and theoretically describe a special micromechanism for the formation of nanocrystallites near the GB steps in Gum Metals. The micromechanism represents a special process of splitting and migration of GBs, driven by both the external stress and stress fields created by the GB steps.

Plastic deformation commonly starts in Gum Metals at applied stresses close to its ideal shear strength and occurs through the formation of giant faults (Fig. 1a) [18–20]. Let us consider the geometric features of intersection of a giant fault and a high-angle GB in a polycrystalline Gum Metal specimen (a two-dimensional schematic illustration is presented in Fig. 1). In the initial state of the system, there are the GB and the giant fault that propagates towards the GB (Fig. 1b). The high-angle GB is assumed to be a symmetric tilt boundary with misorientation angle  $\theta$ . The giant fault plane is perpendicular to the GB plane (Fig. 1b) (in correspondence with experimental data [18–20]). The giant fault carries the plastic shear characterized by the vector  $p_0$ , by which the upper part of the crystal is sheared relative

\* Corresponding author at: Institute of Problems of Mechanical Engineering, Russian Academy of Sciences, Bolshoj 61, Vas. Ostrov, St. Petersburg 199178, Russia. E-mail: [ovidko@nano.ipme.ru](mailto:ovidko@nano.ipme.ru)

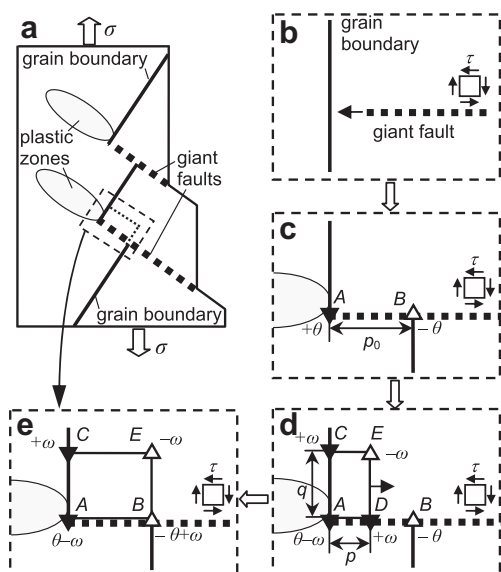


**Figure 1.** Geometry of intersection of giant faults and a grain boundary in Gum Metal. (a) General view. (b) The giant fault moves towards the grain boundary. (c) The giant fault intersects the grain boundary, in which case the grain boundary breaks into two (upper and bottom) fragments, the terminations of which contain wedge disclinations A and B, forming a dipole configuration. The magnitude ( $\theta$ ) of the disclination strengths  $\pm\theta$  is equal to the tilt misorientation ( $\theta$ ) of the grain boundary. The giant fault also spreads into an extended plastic zone in the neighboring grain. The zone is schematically shown as a grey ellipse fragment in the left part of the Gum Metal specimen. (d) The grain boundary fragment AC splits into immobile and mobile grain boundaries, AC and DE, respectively. Stress-driven migration of the mobile grain boundary DE is accompanied by formation of two horizontal grain boundary fragments AD and CE, and thus results in the formation of the new grain ACED. In terms of disclinations, the process under consideration is represented as the generation and evolution of quadrupole of disclinations with strengths  $\pm\omega$ . (e) During evolution of the disclination quadrupole, its horizontal size  $p$  reaches the value of the grain boundary step  $p_0$ . As a result, the defect configuration consisting of two disclination dipoles is formed.

to the bottom part (Fig. 1c). In these circumstances, when the giant fault intersects the GB, the boundary splits into two segments with the distance  $p_0$  between their termination points (lines in a real three-dimensional situation) A and B (Fig. 1c); for further details, see Ref. [21]. The GB termination points A and B serve as wedge disclinations (Fig. 1c) [21]. They are characterized by disclination strengths  $\pm\theta$  and form a dipole configuration (Fig. 1c). (Also, after giant faults intersect with a GB, they spread into extended plastic zones, as experimentally observed in Refs. [19,20] and schematically shown as elliptic-like regions in the left part of the Gum Metal specimen in Fig. 1a and c–e.)

Wedge disclinations of the dipole (Fig. 1c) represent defects that create very high local stresses in the area between them. We think that a partial relaxation of these stresses occurs through the formation of a new nanoscale grain (Fig. 1d and e). More precisely, superposition of the disclination stress fields and the external shear stress  $\tau$  induces splitting of a GB fragment AC (of length  $q$ ) adjacent to the termination point A into the immobile GB fragment (also called AC) and the mobile GB fragment DE that migrates along the giant fault (Fig. 1d).

This splitting results in both change in the misorientation of the upper GB at its fragment AC and the formation of a new nanograin with GBs AC, DE, AD and CE, as shown in Figure 1d. For definiteness, we suppose that all the new GBs DE, AD and CE (Fig. 1d) are symmetric tilt boundaries.

Following the theory [22–25] of stress-driven migration of GBs in bicrystals, the stress-driven migration of the GB DE should be coupled to shear. At the same time, in the case under our consideration, the shear coupled to migration occurs in an internal rectangular region of a solid (but not in a bicrystal). In this case, the plastic shear is limited by the surrounding material and thereby produces a quadrupole of shear-accommodating disclinations at vortices of the internal rectangular region swept by the migrating GB (Fig. 1c) [7,14,16,26]. The latter means that there are non-zero angle gaps  $-\omega$  (the difference in the tilt misorientation between the adjacent GBs) at GB junctions A and E, as well as non-zero angle gaps  $\omega$  (difference in the tilt misorientation) at GB junctions D and C (Fig. 1d). Thus, the splitting and migration process (Fig. 1d) produces a quadrupole of wedge disclinations with strengths  $\pm\omega$  at junctions of GBs of the new nanograin (Fig. 1d).

Note that, together with the wedge disclination with strength  $-\omega$  at point A, another (giant-fault-produced) disclination with strength  $\theta$  is located at the same point. Due to the summing of the strengths of these disclinations, a resultant disclination with strength  $\theta - \omega$  is located at point A. In the further course of plastic deformation, the disclination quadrupole under the shear stress  $\tau$  can grow through an increase in its

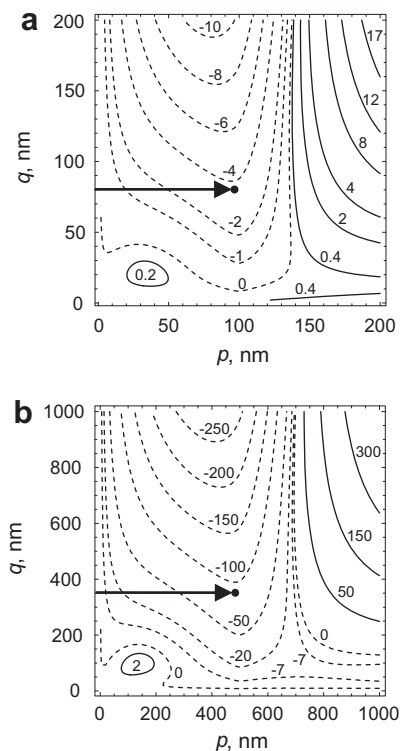


**Figure 2.** Maps of the energy change  $\Delta W(p, q)$ , calculated for  $\tau = 0.5$  GPa,  $\theta = \omega = 0.5$  and (a)  $p_0 = 100$  nm; (b)  $p_0 = 500$  nm. Values of  $\Delta W$  are shown in units of  $10^3 Gb^2 / [2\pi(1 - \nu)]$ .

horizontal size  $p$  and, in the limiting case,  $p$  can reach the size  $p_0$  of the initial disclination dipole  $AB$  (consisting of disclinations  $A$  and  $B$  at the termination points of the fragments of the initial GB). In this case, the configuration of two disclination dipoles is formed, as shown in Figure 1e.

Let us now calculate the energy characteristics of the considered process of GB splitting accompanied by the rearrangement of the disclinations (Fig. 1c and d). The rearrangement in fact represents the formation of the disclination quadrupole  $ACED$  (characterized by the disclination strengths  $\pm\omega$  and sizes  $p$  and  $q$ ) (Fig. 1d). Three new GBs,  $DE$ ,  $AD$  and  $CE$ , are formed (Fig. 1d), and the misorientation angle of the upper GB at its fragment  $AC$  changes. The generation of the disclination quadrupole is specified by the energy change  $\Delta W$ , which can be represented as follows:

$$\Delta W = W_q + W_{int} + \Delta W_{gb} - A. \quad (1)$$

Here  $W_q$  is the proper energy of the disclination quadrupole  $ACED$ ,  $W_{int}$  is the energy of its interaction with the initial disclination dipole  $AB$ ,  $\Delta W_{gb}$  denotes the energy change related to occurrence of new GBs and modification of the pre-existent GB structure, and  $A$  is the work of the external shear stress  $\tau$  spent in the generation and growth of the disclination quadrupole.

The proper energy of the disclination quadrupole in the solid (Gum Metal), modeled as an elastically isotropic medium, is given by the standard formula [27]:

$$W_q = \frac{G\omega^2}{4\pi(1-\nu)} \left[ p^2 \ln \left( 1 + \frac{q^2}{p^2} \right) + q^2 \ln \left( 1 + \frac{p^2}{q^2} \right) \right], \quad (2)$$

where  $G$  is the shear modulus and  $\nu$  is Poisson's ratio. The energy  $W_{int}$  of the interaction between the disclination quadrupole  $ACED$  and the disclination dipole  $AB$  is effectively calculated by the standard method [28] as the work spent in the generation of one defect in the stress field of another defect:

$$W_{int} = \frac{G\theta\omega}{8\pi(1-\nu)} \left[ p^2 \ln \left( 1 + \frac{q^2}{p^2} \right) + q^2 \ln \left( 1 + \frac{p^2}{q^2} \right) + p_0^2 \ln \left( 1 + \frac{q^2}{p_0^2} \right) - (p-p_0)^2 \ln \left( 1 + \frac{q^2}{(p-p_0)^2} \right) - q^2 \ln \frac{(p-p_0)^2 + q^2}{p_0^2 + q^2} \right]. \quad (3)$$

In a first approximation calculation of the energy penalty  $\Delta W_{gb}$ , related to the formation of new GBs and the change in the misorientation angle of the upper GB and its fragment  $AC$ , we exploit the following assumption. We assume that all the GBs (including the GB fragment  $AC$  before and after the splitting process) are characterized by the same specific energy  $\gamma_{gb}$  (per GB area), which does not depend on GB misorientation angles. For definiteness, we consider the nanograin formation process in which the new GB  $AD$  does not replace the relevant part of the giant fault but just grows in parallel with the giant fault plane in its vicinity (Fig. 1d and e). In these circumstances,  $\Delta W_{gb}$  is given as:

$$\Delta W_{gb} = \gamma_{gb}(2p+q) \quad (4)$$

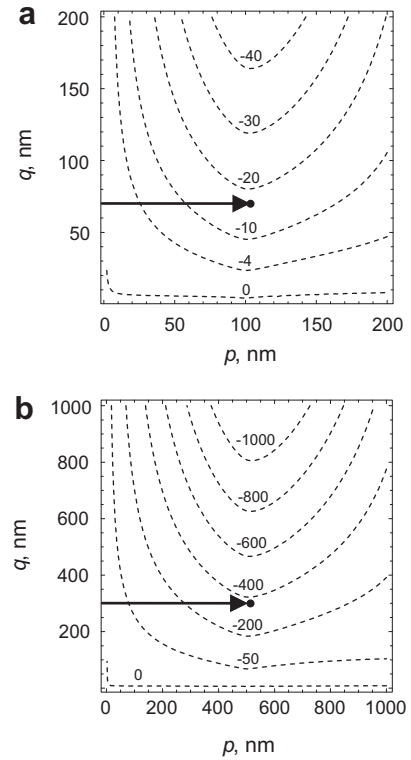


**Figure 3.** Maps of the energy change  $\Delta W(p, q)$ , calculated for  $\tau = 0.5$  GPa,  $\theta = 1$ ,  $\omega = 0.5$  and (a)  $p_0 = 100$  nm; (b)  $p_0 = 500$  nm. Values of  $\Delta W$  are shown in units of  $10^3 Gb^2 / [2\pi(1-\nu)]$ .

The work of the external shear stress  $\tau$ , spent in the generation and growth of the disclination quadrupole, is written as:

$$A = \tau\omega pq. \quad (5)$$

As a corollary, with formulas (1)–(5), we find the following expression for the total energy change  $\Delta W$ :

$$\Delta W = \frac{G\omega^2}{4\pi(1-\nu)} \left\{ \left( 1 + \frac{\theta}{2\omega} \right) \left[ p^2 \ln \left( 1 + \frac{q^2}{p^2} \right) + q^2 \ln \left( 1 + \frac{p^2}{q^2} \right) \right] + \frac{\theta}{2\omega} \left[ p_0^2 \ln \left( 1 + \frac{q^2}{p_0^2} \right) - (p-p_0)^2 \ln \left( 1 + \frac{q^2}{(p-p_0)^2} \right) - q^2 \ln \frac{(p-p_0)^2 + q^2}{p_0^2 + q^2} \right] \right\} + \gamma_{gb}(2p+q) - \tau\omega pq. \quad (6)$$

With formula (6), we calculate the energy change  $\Delta W$  in a Gum Metal specimen having typical values of parameters  $G \approx 25$  GPa and  $\nu \approx 0.3$ . ( $G \approx 25$  GPa is the averaged value corresponding to both experimental data [29] and simulations [30] of elastic constants of Gum Metals showing anisotropic elasticity.) To our knowledge, values of the GB energy in Gum Metals have not been experimentally measured. We therefore suppose  $\gamma_{gb} = 1$  J m<sup>-2</sup>, because this value is typical for general high-angle GBs in high-melting-point metals (including Ti and various Ti-based alloys) [31]. Figures 2 and 3 present the energy maps  $\Delta W(p, q)$ , calculated for the external stress level  $\tau = 0.5$  GPa,  $q > 2$  nm,

$\theta = \omega = 0.5$  (Fig. 2),  $\theta = 1$ ,  $\omega = 0.5$  (Fig. 3),  $p_0 = 100$  nm (Figs. 2a and 3a) and  $p_0 = 500$  nm (Figs. 2b and 3b). The nanograin size (the GB migration length)  $p$  is in the range from 2 nm to  $2p_0$  (Figs. 2 and 3). Note that the atomistic details of the GB splitting dominate at its very initial stage, for  $p < 2$  nm. To describe such details, atomistic simulations are needed which are beyond the scope of our continuum approach. At the same time, the energy maps of the GB splitting and migration (Figs. 2 and 3) in the range of  $p \geq 2$  nm is critical for the splitting to occur, because the very initial stage ( $p < 2$  nm) may occur through the thermally assisted formation of steps at the initial GB if the splitting of the GB at  $p \geq 2$  nm is energetically favorable. In this context, we will focus our analysis to the situation where  $p \geq 2$  nm.

The energy maps show that the generation of the new nanograin *ACED* is energetically favorable in wide ranges of parameters considered here, and the energy reaches its minimum when the horizontal size  $p$  of the nanograin is close or equal to the GB step length  $p_0$  (Fig. 1d). That is, when the GB step *AB* and the associated wedge disclinations are formed due to giant-fault deformation, their elastic energy is effectively released through the formation of the new nanograin *ACED* (Fig. 1d). In the process, delocalization of plastic shear initially localized within the giant fault occurs. More precisely, initial local shear at the giant fault fragment *AB* (Fig. 1c) “extends” within the region *ACEB* due to the GB *DE* migration coupled to shear (Fig. 1e).

Also, according to the energy maps (Figs. 2 and 3), growth of the nanograin through an increase in its vertical size  $q$  is always energetically favorable. The nanograin growth in question is associated with stress-driven migration of GB *CE*. This process can be hampered by structural obstacles (such as the experimentally observed nanometer-sized particles of the omega phase [32]), which are not taken into account in our calculations of the energy maps (Figs. 2 and 3). GBs can also split into two or more GBs. (Our preliminary analysis shows that such splitting processes are energetically favorable.) As a result, a nanocrystal with “spread” GBs can be formed, and this view is supported by experimental documentation [19,20] of gradual changes in the crystal lattice orientation near giant-fault-produced steps of GBs in Gum Metals. Accounting exactly for both the formation of the “spread” GBs and the hampering factors for the GB migration is a complicated problem, the analysis of which will be the subject of further research.

In this paper, we suggest and theoretically describe a special micromechanism for nanograin formation at GB steps produced due to giant-fault deformation in Gum Metals. Within our model, a nanograin results from stress-driven splitting and migration of GBs in the vicinity of the GB steps. This process carries nanoscale plastic flow and delocalizes shear initially concentrated in giant faults. The process is described in terms of disclinations as the generation and growth of a disclination quadrupole (Fig. 1c–e). Our calculations show that the nanograin formation is energetically favorable in wide ranges of parameters of the system under our study (Figs. 2 and 3).

The work was supported, in part (for S.V.B. and I.A.O.), by the Russian Ministry of Education and Science (Contract 14.740.11.0353 and Grant MK-1702.2010.1).

- [1] D. Wolf, V. Yamakov, S.R. Phillpot, A.K. Mukherjee, H. Gleiter, *Acta Mater.* 53 (2005) 1.
- [2] M. Dao, L. Lu, R.J. Asaro, J.T.M. De Hosson, E. Ma, *Acta Mater.* 55 (2007) 4041.
- [3] C.S. Pande, K.P. Cooper, *Progr. Mater. Sci.* 54 (2009) 689.
- [4] C.C. Koch, I.A. Ovid'ko, S. Seal, S. Veprek, *Structural Nanocrystalline Materials: Fundamentals and Applications*, Cambridge University Press, Cambridge, 2007.
- [5] M. Jin, A.M. Minor, E.A. Stach, J.W. Morris Jr., *Acta Mater.* 52 (2004) 5381.
- [6] W.A. Soer, J.Th.M. De Hosson, A.M. Minor, J.W. Morris Jr., E.A. Stach, *Acta Mater.* 52 (2004) 5783.
- [7] M.Yu. Gutkin, I.A. Ovid'ko, *Appl. Phys. Lett.* 87 (2005) 251916.
- [8] D.S. Gianola, S. Van Petegem, M. Legros, S. Brandstetter, H. Van Swygenhoven, K.J. Hemker, *Acta Mater.* 54 (2006) 2253.
- [9] D.S. Gianola, D.H. Warner, J.F. Molinari, K.J. Hemker, *Scripta Mater.* 55 (2006) 649.
- [10] F. Sansoz, V. Dupont, *Appl. Phys. Lett.* 89 (2006) 111901.
- [11] P.L. Gai, K. Zhang, J. Weertman, *Scripta Mater.* 56 (2007) 25.
- [12] M. Legros, D.S. Gianola, K.J. Hemker, *Acta Mater.* 56 (2008) 3380.
- [13] F. Sansoz, V. Dupont, *Acta Mater.* 56 (2008) 6013.
- [14] I.A. Ovid'ko, A.G. Sheinerman, E.C. Aifantis, *Acta Mater.* 56 (2008) 2718.
- [15] T.J. Rupert, D.S. Gianola, Y. Gan, K.J. Hemker, *Science* 326 (2009) 1686.
- [16] I.A. Ovid'ko, N.V. Skiba, A.K. Mukherjee, *Scripta Mater.* 62 (2010) 387.
- [17] S.V. Bobylev, N.F. Morozov, I.A. Ovid'ko, *Phys. Rev. Lett.* 105 (2010) 055504.
- [18] T. Saito, T. Furuta, J.-H. Hwang, S. Kuramoto, K. Nishino, N. Suzuki, R. Chen, A. Yamada, K. Ito, Y. Seno, T. Nonaka, H. Ikehata, N. Nagasako, C. Iwamoto, Y. Ikuhara, T. Sakuma, *Science* 300 (2003) 464.
- [19] S. Kuramoto, T. Furuta, J.-H. Hwang, K. Nishino, T. Saito, *Met. Mater. Trans. A* 37 (2006) 657.
- [20] M.Yu. Gutkin, T. Ishizaki, S. Kuramoto, I.A. Ovid'ko, *Acta Mater.* 54 (2006) 2489.
- [21] M.Yu. Gutkin, T. Ishizaki, S. Kuramoto, I.A. Ovid'ko, N.V. Skiba, *Int. J. Plasticity* 24 (2008) 1333.
- [22] J. Cahn, J.E. Taylor, *Acta Mater.* 52 (2004) 4887.
- [23] Y. Mishin, M. Asta, J. Li, *Acta Mater.* 58 (2010) 1117.
- [24] J. Cahn, Y. Mishin, A. Suzuki, *Acta Mater.* 54 (2006) 4953.
- [25] D. Caillard, F. Momprou, M. Legros, *Acta Mater.* 57 (2009) 2390.
- [26] M.Yu. Gutkin, K.N. Mikaelyan, I.A. Ovid'ko, *Scripta Mater.* 58 (2008) 850.
- [27] A.E. Romanov, V.I. Vladimirov, in: F.R.N. Nabarro (Ed.), *Dislocations in Solids*, vol. 9, Amsterdam, North Holland, 1992, p. 191.
- [28] T. Mura, in: H. Herman (Ed.), *Advances in Material Research*, vol. 3, Interscience, New York, 1968, pp. 1–108.
- [29] R.J. Talling, R.J. Dashwood, M. Jackson, S. Kuramoto, D. Dye, *Scripta Mater.* 59 (2008) 669.
- [30] M. Hara, Y. Shimizu, T. Yano, N. Takesue, T. Furuta, S. Kuramoto, *Int. J. Mater. Res.* 100 (2009) 3.
- [31] L.E. Murr, *Interfacial Phenomena in Metals and Alloys*, Addison-Wesley, Reading, MA, 1975.
- [32] T. Yano, Y. Murakami, D. Shindo, Y. Hayasaka, S. Kuramoto, *Scripta Mater.* 63 (2010) 536.